BIOCHEMISTRY
including biophysical chemistry & molecular biology

Article

pubs.acs.org/biochemistry

Inversion of the Stereochemistry around the Sulfur Atom of the Axial Methionine Side Chain through Alteration of Amino Acid Side Chain Packing in *Hydrogenobacter thermophilus* Cytochrome c_{552} and Its Functional Consequences

Hulin Tai,[†] Ken Tonegawa,[†] Tomokazu Shibata,[†] Hikaru Hemmi,[‡] Nagao Kobayashi,*[,§] and Yasuhiko Yamamoto*[,†]

[†]Department of Chemistry, University of Tsukuba, Tsukuba 305-8571, Japan

[‡]National Food Research Institute, National Agriculture and Food Research Organization (NARO), Tsukuba 305-8642, Japan

[§]Department of Chemistry, Graduate School of Science, Tohoku University, Sendai 980-8578, Japan

Supporting Information

ABSTRACT: In cytochrome *c*, the coordination of the axial Met S_δ atom to the heme Fe atom occurs in one of two distinctly different stereochemical manners, i.e., *R* and *S* configurations, depending upon which of the two lone pairs of the S_δ atom is involved in the bond; hence, the Fe-coordinated S_δ atom becomes a chiral center. In this study, we demonstrated that an alteration of amino acid side chain packing induced by the mutation of a single amino acid residue, i.e., the A73V mutation, in *Hydrogenobacter thermophilus* cytochrome c_{552} (HT) forces the inversion of the stereochemistry around the S_δ atom from the *R* configuration [Travaglini-Allocatelli, C., et al. (2005) *J. Biol. Chem. 280*, 25729−25734] to the *S* configuration. Functional comparison between the wild-type HT and the A73V mutant possessing the *R* and *S* configurations as to the stereochemistry around the S_δ atom, respectively, demonstrated that the redox potential (E_m) of the mutant at pH 6.00 and 25 °C exhibited a positive shift of ∼20 mV relative to that of the wild-type HT, i.e., 245 mV, in an entropic manner. Because these two proteins have similar enthalpically stabilizing interactions, the difference in the entropic contribution to the E_m value between them is likely to be due to the effect of the conformational alteration of the axial Met side chain associated with the inversion of the stereochemistry around the S_δ atom due to the effect of mutation on the internal mobility of the loop bearing the axial Met. Thus, the present study demonstrated that the internal mobility of the loop bearing the axial Met, relevant to entropic control of the redox function of the protein, is affected quite sensitively by the contextual stereochemical packing of amino acid side chains in the proximity of the axial Met.

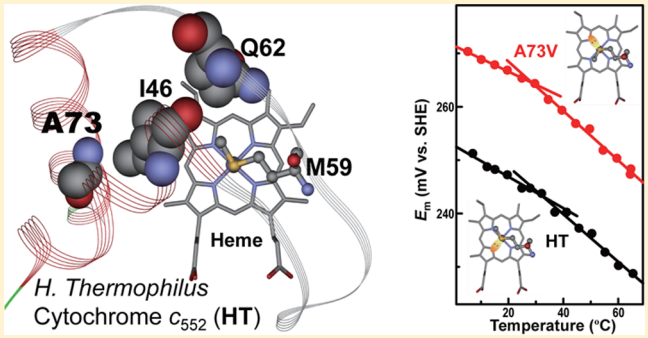

Class I cytochromes *c* (cyts *c*), in which the heme Fe is coordinated to His and Met as axial ligands at the redox center, are some of the best characterized redox active proteins.[1,2] The redox activities of cyts *c* are thought to be regulated by the chemical nature of the redox center because the redox-dependent conformational change has been shown to be quite small.[3−5] The nature of the axial His and Met coordination is a prime determinant of the heme electronic structure relevant to the protein function,[6] and the redox property of the protein has been shown to be regulated through the stability of the Fe−Met coordination bond that is highly sensitive to its physicochemical environment.[7−9]

The conformational freedom of the axial His imidazole in cyts *c* is somewhat restricted because of the covalent attachment of heme to the protein moiety, with the coordination of the His imidazole to the heme Fe atom through the heme attachment motif Cys-x-z-Cys-His (x and z represent arbitrary amino acid residues)[10] and the formation of a hydrogen bond between the His $N_\delta H$ proton and surrounding residues.[4,5,10,11] On the other hand, the coordination of the axial Met S_δ atom to the heme Fe atom occurs in one of two distinctly different stereochemical manners, depending upon which one of the two lone pairs of the S_δ atom is involved in the bond; hence, the Fe-coordinated S_δ atom becomes a chiral center (Figure 1).[3,4,11−14] The two conformations of the axial Met side chain, i.e., the *R* and *S* configurations (Figure 1), are related to each other through inversion of the stereochemistry around the S_δ atom. In

Received: March 28, 2013
Revised: June 20, 2013
Published: June 24, 2013

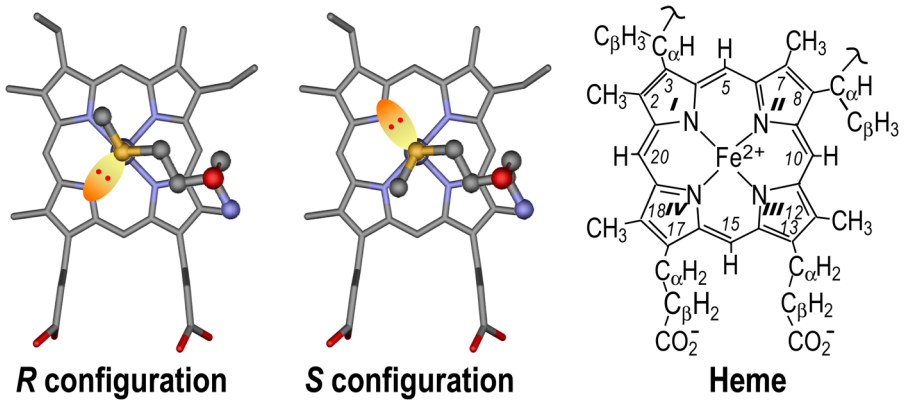

Figure 1. Two different stereochemical manners of coordination of the axial Met S_δ atom to the heme Fe atom, the *R* (left) and *S* (center) configurations. The orientation of the lone pair of the S_δ atom with respect to the heme is also illustrated. The molecular structure and numbering system for the heme are shown at the right.

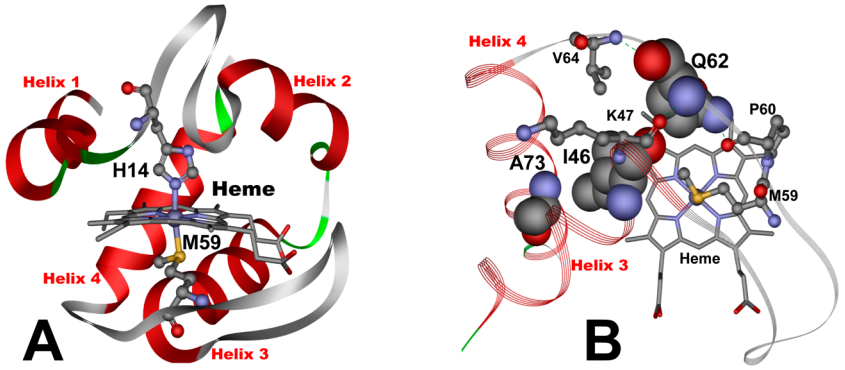

Figure 2. (A) Schematic representation of the structure of *H. thermophilus* cytochrome c_{552} (HT) (PDB entry: 1YNR).[14] The polypeptide chain is illustrated as a ribbon model and the heme as a stick model; axial H14 and M59 are illustrated as ball and stick models. Helices 1−4 are also indicated. (B) Orientation of I46, K47, M59, P60, Q62, V64, and A73 with respect to the heme. I46, Q62, and A73 are shown as space-filling models, and K47, M59, P60, and V64 as ball and stick models. ViewerLite5.0 (Accelrys, Inc.) was used to draw this figure.

addition, the lone pair of the S_δ atom that is not involved in the bond is usually hydrogen bonded to surrounding residues to stabilize the Fe−Met coordination bond.[3,4,11−13] The stereochemistry around the S_δ atom in cyts *c* is species-dependent. Most bacterial cyts *c* exhibit the *S* configuration,[3,12] while the *R* configuration is observed in mitochondrial cyts *c*[4,12] and some bacterial proteins.[13,14]

In the present study, we attempted to invert the stereochemistry around the Fe-coordinated Met S_δ atom of *Hydrogenobacter thermophilus* cytochrome c_{552} (HT)[14,15] (Figure 2A) in order to elucidate the structural factors that determine the conformation of the axial Met side chain and also the effect of the inversion of the stereochemistry around the Fe-coordinated S_δ atom on the protein function. HT is a small monoheme-containing cyt *c* composed of 80 amino acid residues.[15] HT is a rare example of the Fe-coordinated S_δ atom of the axial Met59 not being hydrogen bonded to surrounding residues, although the stereochemistry around the S_δ atom has been shown to adopt the *R* configuration (Figure 2B).[14] We demonstrated here that an alteration of the amino acid side chain packing induced by the mutation of a single amino acid residue, i.e., Ala73, located ∼1 nm from the axial Met59 (Figure 2B),[14] to Val forces the stereochemistry around the S_δ atom to be inverted from the *R* configuration in the wild-type HT to the *S* configuration in the A73V mutant. NMR structural characterization of the A73V mutant and mutation studies on Gln62 of the protein demonstrated that two residues, i.e., Ile46 and Gln62, play important roles in the inversion of the stereochemistry around the axial Met59 S_δ atom upon the A73V mutation. Functional comparison between the wild-type HT and the A73V mutant possessing the *R* and *S* configurations as to the stereochemistry around the S_δ atom, respectively, demonstrated that the redox potential (E_m) of the mutant at pH 6.00 and 25 °C exhibited a positive shift of ∼20 mV relative to that of the wild-type HT, i.e., 245 mV,[9] in an entropic manner. Because these two proteins are thought to have similar enthalpically stabilizing interactions, the difference in the entropic contribution to the E_m value between them could be due to the effect of the conformational alteration of the axial Met side chain associated with the inversion of the stereochemistry around the S_δ atom due to the effect of the mutation on the internal mobility of the loop bearing the axial Met59.

MATERIALS AND METHODS

Protein Samples. The wild-type HT and its mutants were produced using *Escherichia coli* cells and purified as reported previously.[15−17] The oxidized and reduced forms of the proteins were prepared by the addition of a 10-fold molar excess of potassium ferricyanide and a 100-fold excess of disodium dithionite, and by flushing with nitrogen gas, respectively. For NMR samples, the proteins were concentrated to ∼1 mM in an ultrafiltration cell (YM-5, Amicon), and then 10% ^2H_2O or 100% ^2H_2O was added to the protein solutions.

dx.doi.org/10.1021/bi4004028 | *Biochemistry* 2013, 52, 4800−4809

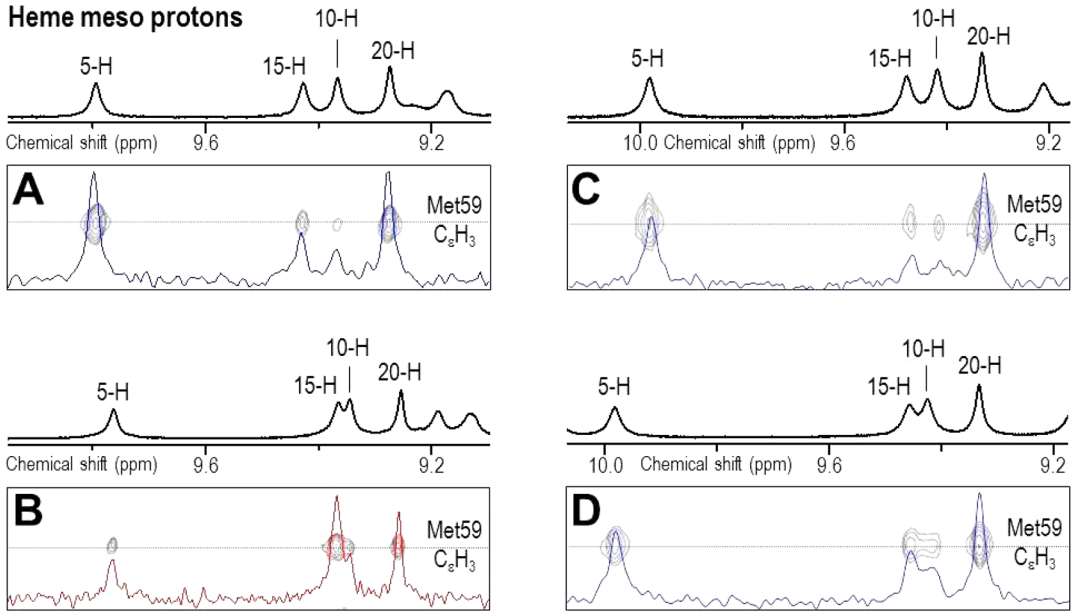

Figure 3. NOESY connectivities between the axial Met59 $C_\varepsilon H_3$ and heme meso protons of the reduced forms of the wild-type HT and mutants at pH 7.0 and 25 °C. (A) HT, (B) A73V mutant, (C) Q62A mutant, and (D) Q62A/A73V double mutant (for the signal assignments, see Figures S2–S6 in the Supporting Information). Slice spectra at the Met59 $C_\varepsilon H_3$ proton signals of the proteins are overlaid on each of the corresponding NOESY spectra (red spectrum for B and blue spectra for A, C, and D).

The pH of each sample was adjusted using 0.2 M KOH or 0.2 M HCl and monitored with a Horiba F-72 pH meter with a Horiba type 9618-10D electrode.

NMR. NMR spectra were recorded on a Bruker Avance 600 FT NMR spectrometer operating at the ^{1}H frequency of 600 MHz. The signal assignments were based on two-dimensional double quantum-filtered chemical shift correlation spectroscopy (DQF-COSY), total COSY (TOCSY), and nuclear Overhauser effect spectroscopy (NOESY) spectra acquired using the standard pulse sequences. To detect connectivities between paramagnetically shifted signals, NOESY spectra with a spectral width of 60 ppm in the t_1 and t_2 dimensions, and 512 and 4096 complex points in the t_1 and t_2 dimensions, respectively, were acquired. TOCSY spectra were obtained with a mixing time of 200 ms, and NOESY spectra with a mixing time of 150 or 200 ms. Before Fourier transformation, a phase-shifted sine-squared window function was applied to both dimensions. Water suppression was performed by the presaturation method or watergate method.[18] Chemical shifts are given in parts per million downfield from sodium 2,2-dimethyl-2-silapentane-5-sulfonate with H_2O as an internal reference. ^{15}N–^{1}H heteronuclear single quantum coherence (HSQC) spectra were recorded using a standard pulse sequence. Spectra were zero-filled to give a final matrix of 2048 × 512 data points and apodized with a 90° shifted sine-bell window function in both dimensions. Assignments of the ^{15}N–^{1}H HSQC cross-peaks of the proteins were made by analyzing ^{15}N-edited NOESY-HSQC and ^{15}N-edited TOCSY-HSQC spectra. The mixing times were 200 and 80 ms for the ^{15}N-edited NOESY-HSQC and ^{15}N-edited TOCSY-HSQC experiments, respectively. Both the ^{1}H and ^{15}N chemical shifts were calibrated against the ^{1}H shift of sodium 2,2-dimethyl-2-silapentane-5-sulfonate.[19]

Cyclic Voltammetry. The procedures used for obtaining cyclic voltammograms for the proteins were essentially the same as those described previously.[20,21] Cyclic voltammetry (CV) experiments were performed with a Potentiostat-Galvanostat PGSTAT12 (Autolab). A glassy carbon electrode (GCE) was polished with a 0.05 μm alumina slurry and then sonicated in deionized water for 1 min. A 1 mM protein solution (2 μL) was spread evenly with a microsyringe on the surface of the GCE. Then the GCE surface was covered with a semipermeable membrane. All E_m values were referenced to a standard hydrogen electrode. The experimental error for E_m was ±2 mV. Variable-temperature experiments were performed using a homebuilt nonisothermal electrochemical cell configuration,[22] in which the temperature of the reference electrode was kept constant. The anodic-to-cathodic peak current ratios obtained at various potential scan rates (1–100 mV s^{-1}) were all ~1. Both the anodic and cathodic peak currents increased linearly as a function of the square root of the scan rate in the range up to 100 mV s^{-1}. Thus, the wild-type HT and its mutants exhibit quasi-reversible redox processes.

Circular Dichroism Spectroscopy. Circular dichroism (CD) spectra were recorded on a JASCO J-820 spectrometer over the spectral range of 200–250 nm and in the temperature range of 30–155 °C with a heating rate of 1 °C min^{-1}, using an airtight pressure-proof cell compartment with quartz windows, as previously described.[23] The temperature at the midpoint of the thermal unfolding was used as the denaturation temperature of the protein (T_m). CD spectra over the spectral range of 635–760 nm of the oxidized proteins were also recorded.

RESULTS

Structural Consequences of the A73V Mutation. The effect of the A73V mutation on the coordination structure of the axial Met59 in the reduced protein has been evaluated through analysis of NOEs between the axial Met and heme meso protons.[24] The NOE connectivities observed for the reduced wild-type HT and A73V mutant are compared in Figure 3 (see also Figure S1 in the Supporting Information). In the spectrum of the wild-type HT, the axial Met59 $C_\varepsilon H_3$ proton signals exhibited strong NOEs to the heme meso 5-H and 20-H protons, clearly indicating that the axial Met59 adopts the *R*

dx.doi.org/10.1021/bi4004028 | *Biochemistry* 2013, 52, 4800–4809

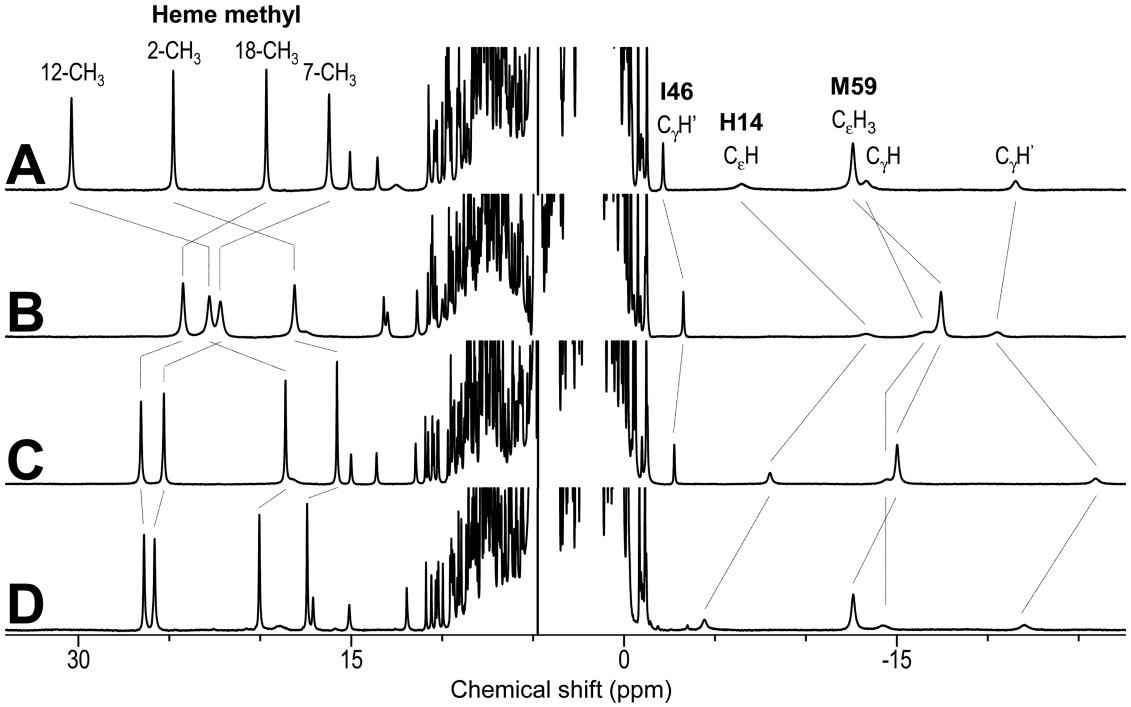

Figure 4. 600 MHz ^{1}H NMR spectra of the oxidized proteins of the wild-type HT and mutants at pH 7.0 and 25 °C. (A) A73V mutant, (B) HT, (C) Q62A mutant, and (D) Q62A/A73V double mutant. Assignments of some signals are indicated with the spectra, and corresponding signals are connected by broken lines. (For the signal assignments, see Figures S10−S19 in the Supporting Information.)

configuration of the axial Met59 S_δ atom (Figure 3A), consistent with the X-ray structure.[14] On the other hand, in the spectrum of the A73V mutant (Figure 3B), the axial Met59 $C_\varepsilon H_3$ proton signals exhibited strong NOEs to heme meso 15-H and 20-H protons, demonstrating that the axial Met59 adopts the *S* configuration of the S_δ atom. Thus, the NOE connectivities clearly demonstrated that the stereochemistry around the axial Met59 S_δ atom in the protein was inverted by the A73V mutation.

The inversion of the stereochemistry around the axial Met59 S_δ atom in the protein was also manifested in the heme methyl proton shift pattern of the oxidized protein. The oxidized A73V mutant exhibited the heme methyl proton shift pattern of 7-CH_3 < 18-CH_3 < 2-CH_3 < 12-CH_3, in order of increasing shift (Figure 4A), whereas the wild-type HT exhibited that of 2-CH_3 < 7-CH_3 < 12-CH_3 < 18-CH_3 (Figure 4B). The heme methyl proton shift pattern observed for the oxidized A73V mutant is consistent with the *S* configuration for the stereochemistry around the axial Met59 S_δ atom (see below).[25] The 4-fold symmetry of the porphyrin π-electron distribution of the heme in a hemoprotein is greatly distorted by the heme−protein interaction in addition to the asymmetric peripheral substitutions. Particularly in the case of the ferric low spin heme complex, the in-plane asymmetry of the heme electronic structure has been shown to be predominantly determined by the orientation of the axial ligands with respect to the heme.[26−28] Considering the stability of the axial His14 coordination structure in the protein,[10,29] the large difference in the in-plane asymmetry of the heme electronic structure between the two proteins can be attributed solely to the alteration of the axial Met59 coordination structure upon the mutation, as has been described previously.[25] In contrast to the case of the oxidized protein, the heme proton shifts of the reduced protein were affected very little by the inversion of the stereochemistry around the axial Met59 S_δ atom (Table 1 and Supporting Information, Figure S2).

The effects of the A73V mutation on the protein structure were manifested in the shift changes of the ^{1}H−^{15}N HSQC cross-peaks of the reduced protein (Figure 5). The main chain amide NH ^{1}H and ^{15}N shifts of the residues at positions 39−51, 59, 62, and 71−77 were greatly affected by the A73V mutation, whereas those of the residues at positions 1−38 were essentially unaffected (Figure 5). There are four helices, i.e., helices 1−4 composed of the residues at positions 2−8, 25−32, 39−48, and 66−78, respectively, in the polypeptide of HT, and roughly speaking, helices 1 and 2 are located on the side of the axial His14, relative to the heme, and helices 3 and 4 on the side of the axial Met59 (Figure 2A). Therefore, the heme is accommodated in the active site of the protein as if it is sandwiched between these two domains of the protein moiety, i.e., helix 1-loop-helix 2 and helix 3-loop-helix 4 domains (Figure 2A). The ^{1}H−^{15}N HSQC comparative study on the reduced wild-type HT and A73V mutant demonstrated that the structural change induced by the A73V mutation is mostly localized in the helix 3-loop-helix 4 domain. According to the X-ray structure of HT,[14] Ala73 is located in the proximity of Val39, Ala43, and Ile46 in helix 3, forming a hydrophobic core at the interface between helices 3 and 4. Therefore, the conformational change of the Val39−Ser51 polypeptide is thought to be induced through structural changes in the interhelical region caused by the A73V mutation, which also influences the conformation of the polypeptide loop near Gln62.

Furthermore, in the ^{1}H NMR spectrum of the reduced A73V mutant, the Ile46 $C_\gamma H_3$ proton signal is resolved at 0.18 ppm, whereas the corresponding signal in the spectrum of the wild-type HT was buried in the diamagnetic envelope where protein signals overlap severely (Table 2 and see Figure S2 in the

dx.doi.org/10.1021/bi4004028 | *Biochemistry* 2013, 52, 4800−4809

Table 1. Chemical Shifts (ppm) of Selected Heme and Axial Met59 Side Chain Proton Signals of Wild-Type HT and Mutants at pH 7.0 and 25 °C

	heme											axial Met59				
reduced form	2-CH_3	7-CH_3	12-CH_3	18-CH_3	3-H_α	3-$C_\beta H_3$	8-H_α	8-$C_\beta H_3$	5-H	10-H	15-H	20-H	C_βH	$C_{\beta'}$H	C_γH	$C_{\gamma'}$H	$C_\varepsilon H_3$
HT	3.67	3.86	3.31	3.44	6.14	1.99	6.22	2.43	9.78	9.42	9.36	9.27	−0.62	−2.61	−1.06	−3.63	−2.90
A73V	3.61	3.82	3.27	3.40	6.11	1.97	6.18	2.40	9.76	9.35	9.37	9.26	−0.80	−2.74	−0.73	−3.77	−2.99
Q62A	3.72	3.89	3.38	3.43	6.26	2.01	6.26	2.54	9.98	9.42	9.47	9.33	−0.56	−2.45	−1.12	−3.48	−2.83
Q62A/A73V	3.70	3.89	3.37	3.41	6.26	2.01	6.25	2.55	9.98	9.42	9.45	9.33	−0.64	−2.44	−0.97	−3.56	−2.86
	heme												axial Met59				
oxidized form	2-CH_3	7-CH_3	12-CH_3	18-CH_3	13-H_α	13-$H_{\alpha'}$	13-H_β	13-$H_{\beta'}$	17-H_α	17-$H_{\alpha'}$	17-H_β	17-$H_{\beta'}$	C_γH	$C_{\gamma'}$H	$C_\varepsilon H_3$		
HT	18.21	22.14	22.96	24.15	9.17	3.64	n.d.	0.99	13.03	2.09	n.d.	1.26	−16.83	−20.27	−17.29		
A73V	25.05	16.17	30.73	19.67	13.78	7.76	0.25	1.31	10.74	−0.45	0.74	0.34	−13.17	−21.58	−12.47		
Q62A	15.78	25.50	18.59	26.79	6.92	1.75	n.d.	0.68	15.14	3.55	n.d.	1.91	−14.47	−26.69	−15.43		
Q62A/A73V	17.37	26.06	19.95	26.63	8.25	2.28	n.d.	0.91	17.24	2.03	n.d.	1.88	−14.34	−22.54	−12.94		

Supporting Information), indicating that the orientation of the Ile46 side chain with respect to the heme was greatly affected by the mutation. The A73V mutation also resulted in sizable shift changes for some of the Ile46 proton signals of the oxidized protein (Table 2). Because the contribution of the contact shift to the paramagnetic shift can be neglected for signals other than those of the heme and the Fe-bound His14 and Met59 side chain protons,[30] the differences in the shifts of the Ile46 proton signals between the oxidized forms of the wild-type HT and the A73V mutant indicated that the orientation of this residue, with respect to the heme, as well as its side chain conformation is greatly affected by the A73V mutation.

Coordination Structure of Axial Met59 in the Q62A and Q62A/A73V Mutants. To elucidate the path of communication via a conformational change of the protein between the side chains of the residue at position 73 and the axial Met59, we investigated the role of Gln62 in determination of the stereochemistry around the axial Met59 S_δ atom through studies on both the Q62A and Q62A/A73V double mutants. According to the X-ray structure of the wild-type HT,[14] Gln62 is located in the proximity of the axial Met59, and the side chain $N_\varepsilon H_2$ protons of Gln62 are hydrogen bonded to carbonyl CO of Pro60 (Figure 2B). The shifts of the Gln62 $N_\varepsilon H_2$ proton signals of the reduced wild-type HT, i.e., 6.36 and 6.65 ppm (see Figure S7 in the Supporting Information), were consistent with the involvement of these NH_2 protons in the formation of the hydrogen bonds with residues other than the axial Met59.

As in the cases of the wild-type HT and A73V mutant, the coordination structures of the axial Met59 residues in the reduced forms of the Q62A and Q62A/A73V mutants were determined through observation of the NOE connectivities between the axial Met59 $C_\varepsilon H_3$ and heme meso protons (Figure 3C,D and Supporting Information, Figure S1). Interestingly, the NOE connectivities observed for both the reduced Q62A and Q62A/A73V mutants were essentially identical to those of the reduced wild-type HT, i.e., the axial Met59 $C_\varepsilon H_3$ proton signals exhibited strong NOEs to the heme meso 5-H and 20-H protons, indicating that the stereochemistry around the axial Met59 S_δ atom in these mutants retains the *R* configuration, as in the wild-type protein.

The oxidized forms of both the Q62A and Q62A/A73V mutants exhibited the heme methyl proton shift pattern of 2-CH_3 < 12-CH_3 < 7-CH_3 < 18-CH_3, in order of increasing shift (Figure 4), as in the case of horse heart cyt *c*,[30] consistent with the *R* configuration for the stereochemistry around the axial Met S_δ atom. The result that the stereochemistry around the axial Met59 S_δ atom in the Q62A mutant was not inverted by the A73V mutation clearly demonstrated that Gln62 is involved in structural communication between the side chains of the residue at position 73 and the axial Met59.

In addition, similar to the spectrum of the reduced A73V mutant, the Ile46 $C_\gamma H_3$ proton signal was resolved at 0.31 ppm in the spectrum of the Q62A/A73V mutant (Figure S2 in the Supporting Information). This result suggested that the orientation of the Ile46 side chain with respect to the heme in the Q62A/A73V mutant is similar to that in the A73V mutant; hence, the effect of the A73V mutation on the Ile46 side chain conformation is independent of the Q62A mutation.

CD Spectra of the Mutants. The CD spectra of the oxidized proteins were analyzed to elucidate how the inversion of the stereochemistry around the axial Met59 S_δ atom is reflected in the spectra (Figure 6). The absorbance at ~690 nm characteristic of an oxidized cyt *c* has been attributed to a

dx.doi.org/10.1021/bi4004028 | *Biochemistry* 2013, 52, 4800−4809

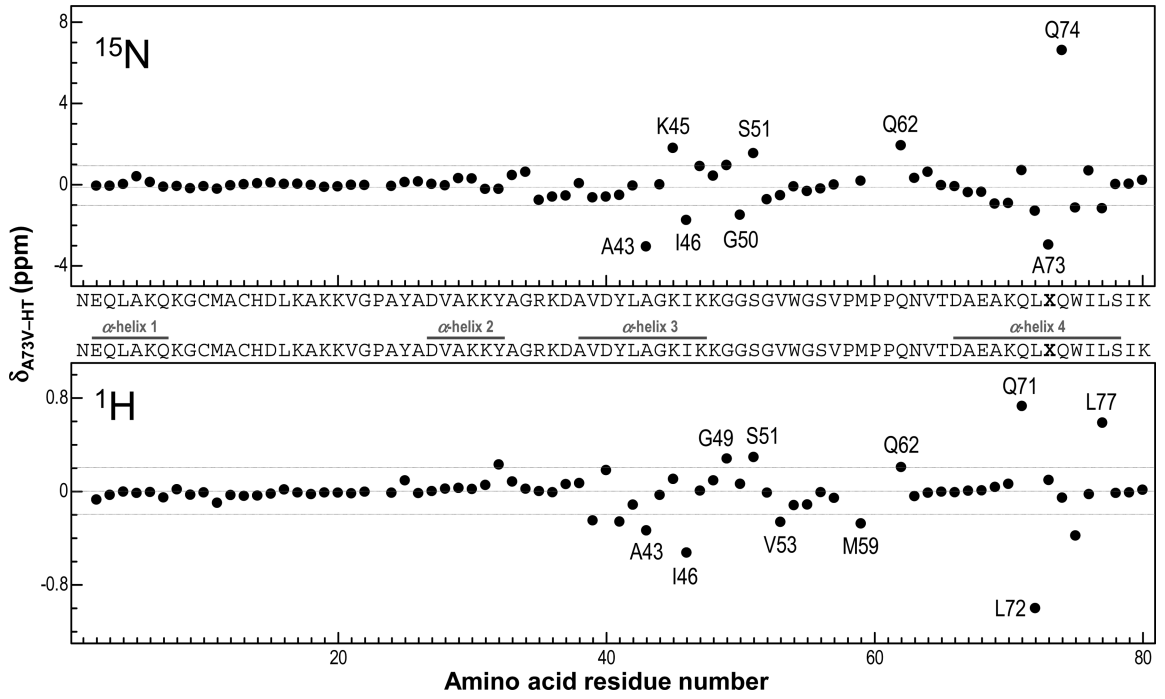

Figure 5. Plots of the shifts (measured in parts per million) for the main chain amide ^{1}H and ^{15}N NMR signals of the A73V mutant in 90% H_2O/10% $^{2}H_2O$, pH 6.0, at 25 °C relative to those of the corresponding shifts of the wild-type HT ($\delta_{A73V-HT}$) against the amino acid residue number. (For the spectra, see Figure S10 in the Supporting Information.) Effects of the A73V mutation on the main chain amide ^{1}H and ^{15}N signals are observed on the residues at positions 39−77.

porphyrin ligand-to-metal charge transfer transition,[31,32] and it has been reported that the stereochemistry around the axial Met S_δ atom in the oxidized cyt *c* is manifested in the sign of the Cotton effect observed in the 690 nm region.[33] As reported previously,[34] in the CD spectrum of the oxidized wild-type HT, no distinct Cotton effect was observed in this region. On the other hand, a weak positive Cotton effect was observed for the oxidized A73V mutant (Figure 6). Furthermore, a faint negative Cotton effect was observed for the oxidized Q62A and Q62A/A73V mutants. Hsu and Woody[35] demonstrated that the heme Cotton effects in hemoproteins are greatly affected by electronic coupling between the heme $\pi-\pi^*$ transition and allowed transistions of nearby chromophores. Namely, the CD spectral comparison among the oxidized forms of the wild-type HT and the three mutants may not be simply interpreted in terms of the stereochemistry around the axial Met59 S_δ atom. However, because the oxidized forms of the wild-type HT and the Q62A and Q62A/A73V mutants all exhibit the *R* configurations, as demonstrated by an X-ray crystallographic study[14] and the NMR results (Figure 3), and the direction of the change of the CD curve of the oxidized A73V mutant in Figure 6 is exactly opposite that of the oxidized Q62A mutant, i.e., the CD spectrum of the oxidized A73V mutant exhibited trough−peak−trough curve in the region of ca. 660−680, 680−700, and 700−760 nm, respectively, while an exactly opposite peak−trough−peak curve was observed in the corresponding regions of the spectrum of the oxidized Q62A mutant, the CD spectral comparison in Figure 6 would suggest that the stereochemistry around the S_δ atom in the A73V mutant alone is much different than those in the other proteins, plausibly the *S* configuration, as indicated by the NMR results in Figure 3. The spectral differences among the wild-type HT and the Q62A and Q62A/A73V mutants represented the high sensitivity of the Cotton effect observed in the 690 nm region to the heme active site structure other than the stereochemistry around the axial Met S_δ atom.

Thermostabilities of the A73V Mutants. The thermostabilities of the oxidized and reduced forms of the A73V mutant at pH 7.0 were analyzed through measurement of CD spectra (200−250 nm) in the temperature range of 30−155 °C (Figure S20 in the Supporting Information). The fraction of the unfolded protein calculated from the CD ellipticity at 222 nm was plotted against temperature, thermal unfolding profiles for the mutant in both redox forms being obtained (Figure 7). Similar plots for the wild-type protein are also illustrated, for comparison, in Figure 7. The T_m values of the oxidized and reduced A73V mutant were determined to be 102.3 and 126.8 °C, respectively (Table 3), and the obtained T_m values were lower by ∼7 and ∼3 °C relative to those of the oxidized and reduced wild-type HT, respectively.

The thermostabilities of the heme active site structures of the oxidized proteins were also analyzed through measurement of ^{1}H NMR spectra at various temperatures (Figure S21 in the Supporting Information). The heme methyl and Met59 proton signals of the oxidized A73V mutant could be observed up to 96 °C (Figures S21 and S22 in the Supporting Information), reflecting the thermostability of its heme active sites. In contrast to the case of the wild-type protein, the anomalous line broadening of the heme methyl and axial Met59 proton signals at low temperatures, due to a dynamic structure transition of the heme active site,[20] was considerably diminished in the spectra of the oxidized A73V mutant (Figure S21 in the Supporting Information).

Temperature Dependence of the E_m Value of the A73V Mutant. The E_m values of the A73V mutant at various temperatures were measured, and the obtained values, together with those of the wild-type protein for comparison, are plotted against temperature (E_m-T plots) in Figure 8. From the E_m-T

dx.doi.org/10.1021/bi4004028 | *Biochemistry* 2013, 52, 4800−4809

Table 2. Chemical Shifts (ppm) of Ile46 Proton Signals of A73V Mutant and Wild-Type HT at pH 7.0 and 25 °C

	amide NH			$C_\alpha H$			$C_\beta H$			$C_\gamma H$			$C_\gamma H_3$			$C_\delta H_3$		
Ile46	A73V	HT	$\delta_{A73V-HT}$	A73V	HT	$\delta_{A73V-HT}$	A73V	HT	$\delta_{A73V-HT}$	A73V	HT	$\delta_{A73V-HT}$	A73V	HT	$\delta_{A73V-HT}$	A73V	HT	$\delta_{A73V-HT}$
δ_{Ox} [a]	8.15	8.62	−0.47	6.60	4.41	2.19	1.73	1.39	0.34	0.20	0.27	−0.07	−2.22	−3.18	0.96	0.88	−0.33	1.21	−0.86	−0.73	0.13
δ_{Red} [b]	7.49	8.02[d]	−0.53	1.57	1.84[d]	−0.27	1.27	1.56[d]	−0.29	n.d.[e]	1.22[d]	n.d.[e]	n.d.[e]	1.35[d]	n.d.[e]	0.18	0.69[d]	−0.51	n.d.[e]	1.21[d]	n.d.[e]
δ_{para} [c]	0.66	0.60		5.03	2.57		0.46	−0.17			−0.95			−4.53		0.70	−1.02			−1.94	

[a]Observed shift of the oxidized form. [b]Observed shift of the reduced form. [c]Paramagnetic shift, i.e., $\delta_{Ox} - \delta_{Red}$. [d]Obtained from ref 16. [e]Not determined.

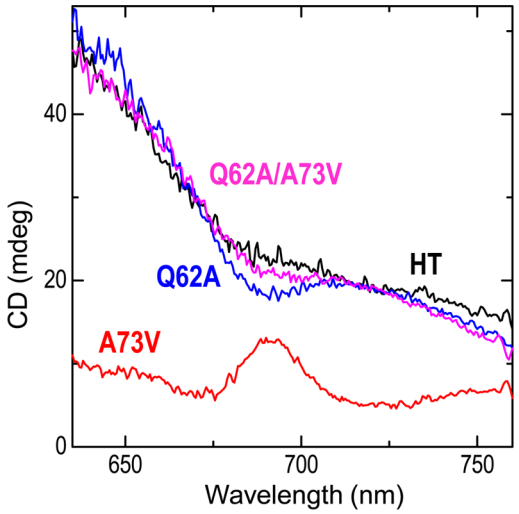

Figure 6. CD spectra of the oxidized proteins of the wild-type HT (black) and A73V (red), Q62A (blue), and Q62A/A73V (pink) mutants at pH 7.00 and 25 °C.

plots, we estimated the enthalpic (ΔH) and entropic (ΔS) contributions to the E_m value (Table 3). The plots for the proteins could be fitted by two straight lines with a transition temperature (T_c) of ∼35 °C (Figure 8).[20,36−39] Hence, two sets of values, $\Delta H^{(low)}$ and $\Delta S^{(low)}$, and $\Delta H^{(high)}$ and $\Delta S^{(high)}$, in the temperature ranges less than T_c and greater than T_c, respectively, were determined for this mutant (Table 3). The anomalous line broadening of the ^{1}H NMR signals arising from the heme methyl and Met59 protons of the HT proteins at low temperatures has been attributed to a temperature-dependent conformational transition between two different protein structures, which differ slightly in the conformation of the loop bearing the Met59 residue.[20] Hence, the appearance of the two different protein structures exhibiting distinctly different thermodynamic parameters resulted in two sets of thermodynamic parameters for the protein. Comparison of the thermodynamic parameters between the wild-type HT and the A73V mutant indicated that the difference in the E_m value between them is due to the entropic contribution rather than the enthalpic contribution. This result is different from those obtained through studies on other HT mutants,[8,9,20,23,36−38] which demonstrated that the E_m value is predominantly controlled through the enthalpic contribution.

DISCUSSION

Effects of the A73V Mutations on the Protein Structure and Coordination Structure of Axial Met59. The inversion of the stereochemistry around the axial Met S_δ atom in the protein upon the A73V mutation, i.e., the *R* configuration in the wild-type HT was converted to the *S* configuration in the mutant, could be attributed to rearrangement of the packing among the side chains of the residue at position 73, Ile46, and Gln62. The side chain of Ala73 is in close contact with that of Ile46, and then the carbonyl CO of the C-terminal neighboring residue of Ile46, i.e., Lys 47, is hydrogen bonded to the main chain NH of Gln62 (Figure 2B).[14] In addition, the carbonyl CO and side chain $N_\varepsilon H_2$ of Gln62 are also hydrogen bonded to the side chain $N_\delta H$ of Val64 and the carbonyl CO of Pro60, respectively, to stabilize the conformation of the polypeptide loop near Gln62.[14] The upfield shift changes observed for the assigned Ile46 proton

dx.doi.org/10.1021/bi4004028 | *Biochemistry* 2013, 52, 4800−4809

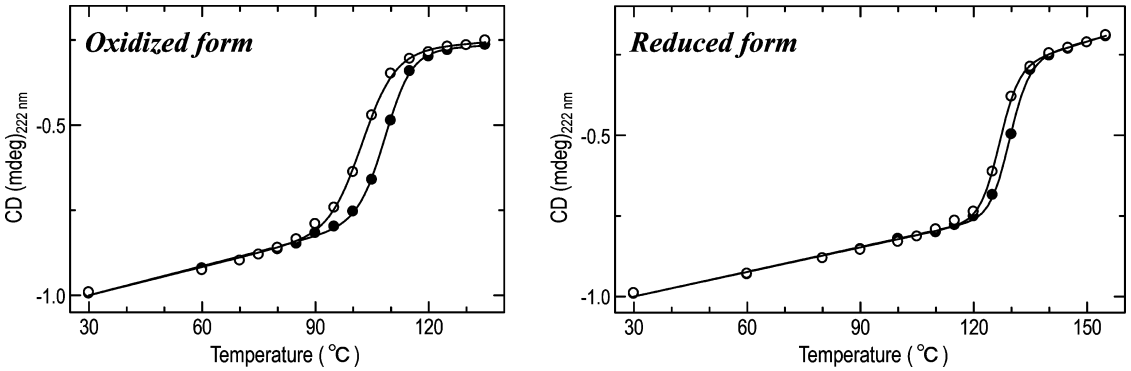

Figure 7. Unfolding profiles of the oxidized (left) and reduced (right) forms of the A73V mutant (open circles) at pH 7.0 (for the spectra, see Figure S20 in the Supporting Information). The plots for the wild-type HT (closed circles) at pH 7.0[37] are also shown for comparison.

Table 3. Denaturation Temperatures, Redox Potentials, and Thermodynamic Parameters of the Redox Reaction for the Wild-Type HT and A73V Mutant

	T_m[a] (°C)				ΔH[f] (kJ mol^{-1})		ΔS[g] (J K^{-1} mol^{-1})	
	Ox[b]	Red[c]	ΔT_m[d] (°C)	E_m[e] (mV)	low	high	low	high
HT[h]	109.8	129.7	19.9	245.0	−32.2	−37.5	−28.4	−45.7
A73V	102.3	126.8	24.5	265.3	−32.6	−38.1	−23.6	−41.7

[a]Denaturation temperature determined at pH 7.0. Experimental error was ±0.2 °C. [b]Oxidized form. [c]Reduced form. [d]Difference in the T_m value between the two redox forms of the protein. [e]Redox potential measured at pH 6.0 and 25 °C. Experimental error was ±2 mV. [f]Enthalpic contribution to the E_m value. Experimental error was ±2 kJ mol^{-1}. [g]Entropic contribution to the E_m value. Experimental error was ±3 J K^{-1} mol^{-1}. [h]Obtained from ref 20.

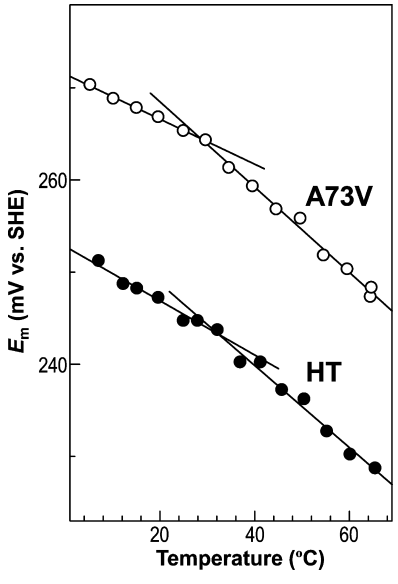

Figure 8. Plots of the redox potential (E_m) against temperature for the A73V mutant at pH 6.0. The plots for the wild-type HT at pH 6.0[20] are also shown for comparison. The plots of the mutant could be also fitted by two straight lines with a transition temperature of ~35 °C.

signals of the reduced protein upon the introduction of the A73V mutation into both the wild-type HT and the Q62A mutant (Table 2 and Supporting Information, Figure S2) indicated the orientation of Ile46, with respect to the heme, as well as its side chain conformation is affected by the A73V mutation. Furthermore, from the results of studies on the Q62A and Q62A/A73V mutants, it was demonstrated that Gln62 plays an essential role in the inversion of the stereochemistry around the axial Met59 S_δ atom upon the A73V mutation. Consequently, it is concluded that the displacement of Ile46 because of the A73V mutation leads to alteration of the contact between the side chains of Met59 and Gln62, which in turn results in the inversion of the stereochemistry around the axial Met59 S_δ atom from the *R* configuration to the *S* configuration.

The Fe-bound Met S_δ atom in cyts *c* is generally hydrogen bonded to a nearby residue, and hence the Fe−Met coordination bond, together with the conformation of the Met side chain, is stabilized by the hydrogen bond. In the case of HT, although the side chain $N_\varepsilon H_2$ group of Gln62 is a potential candidate for a hydrogen bond donor for the Fe-coordinated Met59 S_δ atom, analysis of the shifts of the Gln62 $N_\varepsilon H_2$ proton signals of the reduced wild-type HT, i.e., 6.36 and 6.65 ppm (Figure S7 in the Supporting Information), indicated that the $N_\varepsilon H_2$ group is not hydrogen bonded to the axial Met59 S_δ atom, but to another hydrogen bond acceptor, possibly the carbonyl CO of Pro60, as revealed by an X-ray crystallographic study.[14] The reduced A73V mutant exhibited shifts of 6.40 and 6.75 ppm for the Gln62 $N_\varepsilon H_2$ protons (Figure S8 in the Supporting Information), which are similar to those of the reduced wild-type HT. These results confirmed that the hydrogen bond network of the Gln62 side chain amide group is not affected by the A73V mutation. Consequently, this study demonstrated that the stereochemistry around the axial Met59 S_δ atom in the protein was determined solely by the contextual stereochemical packing of amino residues in the protein interior.

Functional Consequences of the Inversion of the Stereochemistry around the Axial Met59 S_δ Atom. Functional comparison between the wild-type HT and the A73V mutant provided clues to elucidate the relationship between the protein function and the stereochemistry around the axial Met59 S_δ atom. We demonstrated previously that the E_m value of a protein is controlled through the overall protein stability.[8,9,37,38] The T_m values of the oxidized and reduced

dx.doi.org/10.1021/bi4004028 | *Biochemistry* 2013, 52, 4800−4809

A73V mutant were lower by ∼7 and ∼3 °C, respectively, relative to those of the corresponding redox forms of the wild-type HT (Table 3). These results indicated that the A73V mutation slightly decreased the stabilities of both the oxidized and reduced proteins and that the decrease in the stability caused by the mutation was larger for the former than for the latter. Consequently, as expected from the larger difference in the thermodynamic stability between the two different redox forms for the A73V mutant than the wild-type HT, the mutant exhibited a positive shift of ∼20 mV relative to that of the wild-type protein, also consistent with our previous finding that a protein with higher stability in its oxidized form exhibits a lower E_m value.[8,9,37,38] Furthermore, this study demonstrated that the E_m value of the protein is affected only slightly by the inversion of the stereochemistry around the axial Met59 S_δ atom.

The thermodynamic analysis of the E_m values of the proteins indicated that the positive shift of the E_m value of the A73V mutant is due to the ΔS contribution rather than the ΔH contribution. As schematically illustrated in Figure 2B, there is a void space near pyrrole IV (Figure 1) on the side of the axial Met59 in the wild-type HT.[14] In the A73V mutant, this void space is expected to be partially filled by the Met59 $C_\varepsilon H_3$ group, which is also expected to be in close contact with the polypeptide loop near Gly49 and Gly50.[14] Therefore, the internal mobility of the loop bearing the axial Met59 in the protein is likely to be restrained through an increase in the van der Waals contact with the Met59 side chain as a result of the conformational change of its side chain due to the inversion of the stereochemistry around the S_δ atom upon the A73V mutation. The decrease in the internal mobility of the loop bearing the axial Met59 upon the A73V mutation is supported by the result that the temperature-dependent line broadening of the heme methyl and axial Met59 side chain proton signals of the oxidized wild-type HT was considerably diminished by the mutation. Consequently, the entropy of the oxidized protein exhibiting intrinsically greater internal mobility is expected to be more significantly reduced by the A73V mutation than that of the reduced form, leading to a decrease in the $|\Delta S|$ value, as observed in this study (Table 3).

Lazaridis et al.[40] discussed the possibility of entropic stabilization of proteins and pointed out that increasing entropy through promotion of the internal mobility of a protein could enhance its stability, although entropy−enthalpy compensation is expected to yield a corresponding unfavorable increase in enthalpy.[41] The wild-type HT and A73V mutant, however, are thought to have similar enthalpically stabilizing interactions, and hence the decreased protein stability of the A73V mutant, as manifested in the T_m results, could be due to the decrease in the internal mobility of the loop bearing the axial Met59. Thus, this study revealed that the stereochemistry around the Fe-coordinated Met S_δ atom regulates the E_m value of cyt *c* through the internal mobility of the loop bearing the axial Met and that the E_m value of the protein is affected only slightly by the stereochemistry around the axial Met59 S_δ atom.

■ ASSOCIATED CONTENT

Supporting Information

NOESY connectivities between the axial Met59 side chain and heme meso protons; 600 MHz ^{1}H NMR spectra and portions of NOESY spectra of the reduced forms of the wild-type HT, A73V, Q62A, and Q62A/A73V at pH 7.0 and 25 °C; ^{1}H−^{15}N HSQC spectra, with overlays of the two spectra, of the reduced forms of the wild-type HT and A73V mutant in 90% H_2O/10% ^2H_2O, pH 6.0, at 25 °C; portions of NOESY and ^{1}H−^{1}H COSY spectra of the oxidized forms of the wild-type HT, A73V, Q62A, and Q62A/A73V in 100% ^2H_2O, pH 7.0, at 25 °C; temperature-dependent CD spectra, 200−250 nm, of the oxidized and reduced forms of the A73V mutant at pH 7.0; temperature-dependent 600 MHz ^{1}H NMR spectra of the oxidized forms of the wild-type HT and A73V mutant in 100% ^2H_2O, pH 7.0; Curie plots, observed ^{1}H shifts versus reciprocal of absolute temperature, for the heme methyl, axial Met59, and axial His14 protons of the oxidized forms of the wild-type HT and A73V mutant in 100% ^2H_2O, pH 7.0. This material is available free of charge via the Internet at http://pubs.acs.org.

■ AUTHOR INFORMATION

Corresponding Author

*Y.Y.: phone/fax, +81-29-853-6521; e-mail, yamamoto@chem.tsukuba.ac.jp. N.K.: phone/fax, +81-22-795-7719; e-mail, nagaok@m.tohoku.ac.jp.

Funding

This work was supported by a Grant-in-Aid for Scientific Research on Innovative Areas (21108505, "π-Space") from the Ministry of Education, Culture, Sports, Science and Technology, Japan, the Yazaki Memorial Foundation for Science and Technology, and the NOVARTIS Foundation (Japan) for the Promotion of Science.

Notes

The authors declare no competing financial interest.

■ ACKNOWLEDGMENTS

The ^{1}H NMR spectra were recorded on a Bruker AVANCE-600 spectrometer at the Chemical Analysis Center, University of Tsukuba.

■ ABBREVIATIONS

cyt *c*, cytochrome *c*; HT, *H. thermophilus* cytochrome c_{552}; E_m, redox potential; DQF-COSY, two-dimensional double quantum-filtered chemical shift correlation spectroscopy; TOCSY, total COSY; NOESY, two-dimensional nuclear Overhauser effect spectroscopy; HSQC, ^{15}N/^{1}H heteronuclear single quantum coherence; CV, cyclic voltammetry; GCE, glassy carbon electrode; CD, circular dichroism; T_m, denaturation temperature of protein; E_m−T plots, plots of redox potentials of proteins against temperature; T_c, transition temperature

■ REFERENCES

(1) Moore, G. R., and Pettigrew, G. W. (1990) *Cytochromes c: Evolutionary, Structural, and Physicochemical Aspects*, Springer-Verlag, Berlin.

(2) Scott, R. A., and Mauk, A. G., Eds. (1996) *Cytochrome c: A Multidisciplinary Approach*, University Science Books, Sausalito, CA.

(3) Matsuura, Y., Takano, T., and Dickerson, R. E. (1982) Structure of cytochrome c_{551} from *Pseudomonas aeruginosa* refined at 1.6 Å resolution and comparison of the two redox forms. *J. Mol. Biol. 156*, 389−409.

(4) Berghuis, A. M., and Brayer, G. D. (1992) Oxidation state-dependent conformational changes in cytochrome *c*. *J. Mol. Biol. 223*, 959−976.

(5) Brayer, G. D., and Murphy, M. E. P. (1996) in *Cytochrome c: A Multidisciplinary Approach* (Scott, R. A., and Mauk, A. G., Eds.) pp 103−166, University Science Books, Sausalito, CA.

(6) Shokhirev, N. V., and Walker, F. A. (1998) The effect of axial ligand plane orientation on the contact and pseudocontact shifts of low-spin ferriheme proteins. *J. Biol. Inorg. Chem.* 3, 581−594.

(7) Yamamoto, Y., Terui, N., Tachiiri, N., Minakawa, K., Matsuo, H., Kameda, T., Hasegawa, J., Sambongi, Y., Uchiyama, S., Kobayashi, Y., and Igarashi, Y. (2002) Influence of amino acid side chain packing on Fe−methionine coordination in thermostable cytochrome *c*. *J. Am. Chem. Soc. 124*, 11574−11575.
(8) Terui, N., Tachiiri, N., Matsuo, H., Hasegawa, J., Uchiyama, S., Kobayashi, Y., Igarashi, Y., Sambongi, Y., and Yamamoto, Y. (2003) Relationship between redox function and protein stability of cytochromes *c*. *J. Am. Chem. Soc. 125*, 13650−13651.
(9) Takayama, S. J., Mikami, S., Terui, N., Mita, H., Hasegawa, J., Sambongi, Y., and Yamamoto, Y. (2005) Control of the redox potential of *Pseudomonas aeruginosa* cytochrome c_{551} through the Fe−Met coordination bond strength and pK_a of a buried heme propionic acid side chain. *Biochemistry 44*, 5488−5494.
(10) Low, D. W., Gray, H. B., and Duus, J. Ø. (1997) Paramagnetic NMR spectroscopy of microperoxidase-8. *J. Am. Chem. Soc. 119*, 1−5.
(11) Bushnell, G. W., Louie, G. V., and Brayer, G. D. (1990) High-resolution three-dimensional structure of horse heart cytochrome *c*. *J. Mol. Biol. 214*, 585−595.
(12) Timkovich, R., Cai, M., Zhang, B., Arciero, D. M., and Hooper, A. B. (1994) Characteristics of the paramagnetic ^{1}H-NMR spectra of the ferricytochrome c-551 family. *Eur. J. Biochem. 226*, 159−168.
(13) Benning, M. M., Wesenberg, G., Caffrey, M. S., Bartsch, R. G., Meyer, T. E., Cusanovich, M. A., Rayment, I., and Holden, H. M. (1991) Molecular structure of cytochrome c_2 isolated from *Rhodobacter capsulatus* determined at 2.5 Å resolution. *J. Mol. Biol. 220*, 673−685.
(14) Travaglini-Allocatelli, C., Gianni, S., Dubey, V. K., Borgia, A., Di Matteo, A., Bonivento, D., Cutruzzola, F., Bren, K. L., and Brunori, M. (2005) An obligatory intermediate in the folding pathway of cytochrome c_{552} from *Hydrogenobacter thermophilus*. *J. Biol. Chem. 280*, 25729−25734.
(15) Sanbongi, Y., Ishii, M., Igarashi, Y., and Kodama, T. (1989) Amino acid sequence of cytochrome c-552 from a thermophilic hydrogen-oxidizing bacterium, *Hydrogenobacter thermophilus*. *J. Bacteriol. 171*, 65−69.
(16) Hasegawa, J., Yoshida, T., Yamazaki, T., Sambongi, Y., Yu, Y., Igarashi, Y., Kodama, T., Yamazaki, K., Kyogoku, Y., and Kobayashi, Y. (1998) Solution structure of thermostable cytochrome *c*-552 from *Hydrogenobacter thermophilus* determined by ^{1}H-NMR spectroscopy. *Biochemistry 37*, 9641−9649.
(17) Hasegawa, J., Shimahara, H., Mizutani, M., Uchiyama, S., Arai, H., Ishii, M., Kobayashi, Y., Ferguson, S. J., Sambongi, Y., and Igarashi, Y. (1999) Stabilization of *Pseudomonas aeruginosa* cytochrome c_{551} by systematic amino acid substitutions based on the structure of thermophilic *Hydrogenobacter thermophilus* cytochrome c_{552}. *J. Biol. Chem. 274*, 37533−37537.
(18) Piotte, M., Saudek, V., and Sklená, V. (1992) Gradient-tailored excitation for single-quantum NMR spectroscopy of aqueous solutions. *J. Biomol. NMR 2*, 661−665.
(19) Wishart, D. S., Bigam, C. G., Yao, J., Abildgaard, F., Dyson, H. J., Oldfield, E., Markley, J. L., and Sykes, B. D. (1995) ^{1}H, ^{13}C, and ^{15}N chemical shift referencing in biomolecular NMR. *J. Biomol. NMR 6*, 135−140.
(20) Takayama, S. J., Takahashi, Y., Mikami, S., Irie, K., Kawano, S., Yamamoto, Y., Hemmi, H., Kitahara, R., Yokoyama, S., and Akasaka, K. (2007) Local conformational transition of *Hydrogenobacter thermophilus* cytochrome c_{552} relevant to its redox potential. *Biochemistry 46*, 9215−9224.
(21) Lojou, E., and Bianco, P. (2000) Membrane electrodes can modulate the electrochemical response of redox potentials−Direct electrochemistry of cytochrome *c*. *J. Electroanal. Chem. 485*, 71−80.
(22) Battistuzzi, G., Borsari, M., Loschi, L., Menziani, M. C., De Rienzo, F., and Sola, M. (2001) Control of metalloprotein reduction potential: The role of electrostatic and solvation effects probed on plastocyanin mutants. *Biochemistry 40*, 6422−6430.
(23) Uchiyama, S., Ohshima, A., Nakamura, S., Hasegawa, J., Terui, N., Takayama, S. J., Yamamoto, Y., Sambongi, Y., and Kobayashi, Y. (2004) Complete thermal-unfolding profiles of oxidized and reduced cytochromes *c*. *J. Am. Chem. Soc. 126*, 14684−14685.
(24) Senn, H., and Wüthrich, K. (1985) Amino acid sequence, haem-iron coordination geometry and functional properties of mitochondrial and bacterial *c*-type cytochromes. *Q. Rev. Biophys. 18*, 111−134.
(25) Tachiiri, N., Hemmi, H., Takayama, S. J., Mita, H., Hasegawa, J., Sambongi, Y., and Yamamoto, Y. (2004) Effects of axial methionine coordination on the in-plane asymmetry of the heme electronic structure of cytochrome *c*. *J. Biol. Inorg. Chem. 9*, 733−742.
(26) La Mar, G. N., Satterlee, J. D., and de Ropp, J. S. (2000) Nuclear magnetic resonance of hemoproteins. In *The Porphyrin Handbook* (Kadish, K., Smith, K. M., and Guilard, R., Eds.) pp 185−298, Academic Press, New York.
(27) Bertini, I., and Luchinat, C. (1986) *NMR of Paramagnetic Molecules in Biological Systems*, pp 19−46, The Benjamin/Cummings Publishing Co., Menlo Park, CA.
(28) Yamamoto, Y. (1998) NMR study of active sites in paramagnetic hemoproteins. *Annu. Rep. NMR Spectrosc. 36*, 1−77.
(29) Mondelli, R., Scaglioni, L., Mazzini, S., Bolis, G., and Ranghino, G. (2000) 3D structure of microperoxidase-11 by NMR and molecular dynamic studies. *Magn. Reson. Chem. 38*, 229−240.
(30) Feng, Y., Roder, H., and Englander, S. W. (1990) Redox-dependent structure change and hyperfine nuclear magnetic resonance shifts in cytochrome *c*. *Biochemistry 29*, 3494−3504.
(31) Eaton, W. A., and Hochstrasser, R. M. (1967) Electronic spectrum of single crystals of ferricytochrome-*c*. *J. Chem. Phys. 46*, 2533−2539.
(32) Makinen, M. W., and Churg, A. K. (1983) Structural and analytical aspects of the electronic spectra of hemeproteins. In *Iron Porphyrins, Part I* (Lever, A. B. P., and Gray, H. B., Eds.) pp 141−235, Addison-Wesley Publishing Co., Reading, MA.
(33) Keller, R. M., and Wüthrich, K. (1978) Assignment of the heme c resonances in the 360 MHz ^{1}H NMR spectrum of cytochrome *c*. *Biochim. Biophys. Acta 533*, 195−208.
(34) Zhong, L., Wen, X., Rabinowitz, T. M., Russell, B. S., Karan, E. F., and Bren, K. L. (2004) Heme axial methionine fluxionality in *Hydrogenobacter thermophilus* cytochrome c_{552}. *Proc. Natl. Acad. Sci. U.S.A. 101*, 8637−8642.
(35) Hsu, M.-C., and Woody, R. W. (1971) The origin of the heme Cotton effects in myoglobin and hemoglobin. *J. Am. Chem. Soc. 93*, 3515−3525.
(36) Takahashi, Y., Takayama, S. J., Mikami, S., Mita, H., Sambongi, Y., and Yamamoto, Y. (2006) Influence of a single amide group on the redox function of *Pseudomonas aeruginosa* cytochrome c_{551}. *Chem. Lett. 35*, 528−529.
(37) Takahashi, Y., Sasaki, H., Takayama, S. J., Mikami, S., Kawano, S., Mita, H., Sambongi, Y., and Yamamoto, Y. (2006) Further enhancement of the thermostability of *Hydrogenobacter thermophilus* cytochrome c_{552}. *Biochemistry 45*, 11005−11011.
(38) Tai, H., Irie, K., Mikami, S., and Yamamoto, Y. (2011) Enhancement of the thermostability of *Hydrogenobacter thermophilus* cytochrome c_{552} through introduction of an extra methylene group into its hydrophobic protein interior. *Biochemistry 50*, 3161−3169.
(39) Tai, H., Mikami, S., Irie, K., Watanabe, N., Shinohara, N., and Yamamoto, Y. (2010) Role of a highly conserved electrostatic interaction on the surface of cytochrome *c* in control of the redox function. *Biochemistry 49*, 42−48.
(40) Lazaridis, T., Lee, I., and Karplus, M. (1997) Dynamics and unfolding pathways of a hyperthermophilic and a mesophilic rubredoxin. *Protein Sci. 6*, 2589−2605.
(41) Lumry, R., and Rajender, S. (1970) Enthalpy−entropy compensation phenomena in water solutions of proteins and small molecules: A ubiquitous property of water. *Biopolymers 9*, 1125−1227.